



A simulation methodology for superconducting qubit readout fidelity

Hiu Yung Wong^a, Prabjot Dhillon^a, Kristin M. Beck^b, Yaniv J. Rosen^b

^a Electrical Engineering, San Jose State University, CA, USA

^b Lawrence Livermore National Laboratory, Livermore, CA, USA

ARTICLE INFO

Handling Editor Francisco Gamiz

Keywords:

HFSS
Matlab
Noise
Qubit readout
Quantum computing
Resonator
Superconducting Qubit

ABSTRACT

Qubit readout is a critical part of any quantum computer including the superconducting-qubit-based one. The readout fidelity is affected by the readout pulse width, readout pulse energy, resonator design, qubit design, qubit-resonator coupling, and the noise generated along the readout path. It is thus important to model and predict the fidelity based on various design parameters along the readout path. In this work, a simulation methodology for superconducting qubit readout fidelity is proposed and implemented using Matlab and Ansys HFSS to allow co-optimization in the readout path. As an example, parameters are taken from an actual superconducting-qubit-based quantum computer. Without any calibrations, the model is able to predict the readout error of the system as a function of the readout pulse power. It is found that the system can still maintain high fidelity even if the input power is reduced by 7 dB. This can be used to guide the design and optimization of a superconducting qubit readout system.

1. Introduction

Superconducting qubits are one of the most promising quantum computing architectures [1]. While a qubit needs to have enough isolation to achieve a long coherence time, it should also be allowed to interact with the outside world for the readout operation. Often, a resonator is coupled to a qubit to allow dispersive readout, in which the resonator will experience a resonance frequency shift depending on the final state of the qubit [2]. This frequency shift is called the Cross-Kerr, χ . The larger the χ , the easier it is to distinguish the qubit's $|0\rangle$ and $|1\rangle$ states. However, this will also result in a shorter coherence time. The distinguishability of the $|0\rangle$ and $|1\rangle$ states also depends on the readout pulse power and duration, the resonator scattering matrix, and the noise from the readout circuit. Therefore, it is important to co-optimize the resonator design, qubit-resonator coupling, and reading pulse length and power with the noise taken into account.

In this paper, a simulation framework and methodology are proposed and implemented using Matlab and Ansys HFSS. It is then used to predict how the fidelity changes with the readout pulse power.

2. The qubit readout system

Fig. 1 shows the experimental hardware system used in this paper. Quantum Machine OPX is used as the control hardware, with a single sideband mixer and stable RF source used to upconvert the outputs to

the qubit and readout frequencies [3]. A readout pulse of -47dBm nominal power and $3.5\ \mu\text{s}$ duration (t_p) at $7.246245\ \text{GHz}$ is used. The nominal power is the power currently being used in the system. After three attenuation stages ($-60\ \text{dB}$ in total) and the attenuation due to the cables (measured to be $-16\ \text{dB}$), the pulse reaches the input port (port 1, where the pulse becomes -123dBm) of the resonator coupled to a qubit at 10mK . The qubit is tantalum-based with a long coherence time ($\sim 0.25\ \text{ms}$) [4]. The signal from the output port (port 2) of the resonator is then amplified by a Traveling Wave Parametric Amplifier (TWPA) ($+20\ \text{dB}$) at 10mK , a High Electron Mobility Transistor (HEMT) amplifier at $4\ \text{K}$ ($+40\ \text{dB}$), and a $300\ \text{K}$ amplifier ($+40\ \text{dB}$). Quadrature measurement is performed on the amplified output signal, which represents the S_{21} of the resonator/qubit system, to distinguish the qubit $|0\rangle$ and $|1\rangle$ states. The χ of the system is measured to be $114\ \text{kHz}$.

3. Simulation methodology

Fig. 2 shows the simulation framework. The framework uses Ansys HFSS [5] to perform the scattering matrix simulation of the resonator (to be detailed in the next section). The S_{21} obtained is then fed into a MATLAB program to simulate the readout process. There are three major noise sources. The first one is the quantum noise due to the photon number fluctuation after the resonator. The second one is the noise due to the TWPA. Since TWPA is a quantum-limited amplifier, therefore, at the best case, it only reduces the signal-to-noise ratio by half when the

E-mail address: hiuyung.wong@sjsu.edu (H.Y. Wong).

<https://doi.org/10.1016/j.sse.2022.108582>

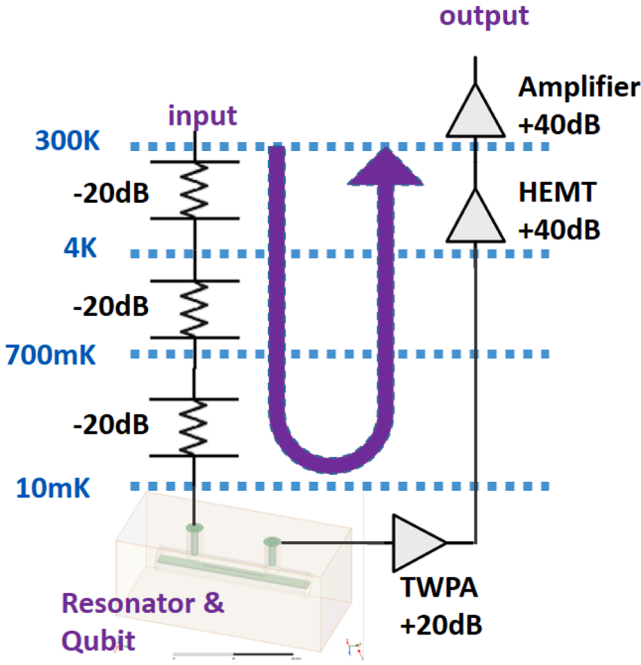


Fig. 1. The qubit system used. The readout path is highlighted.

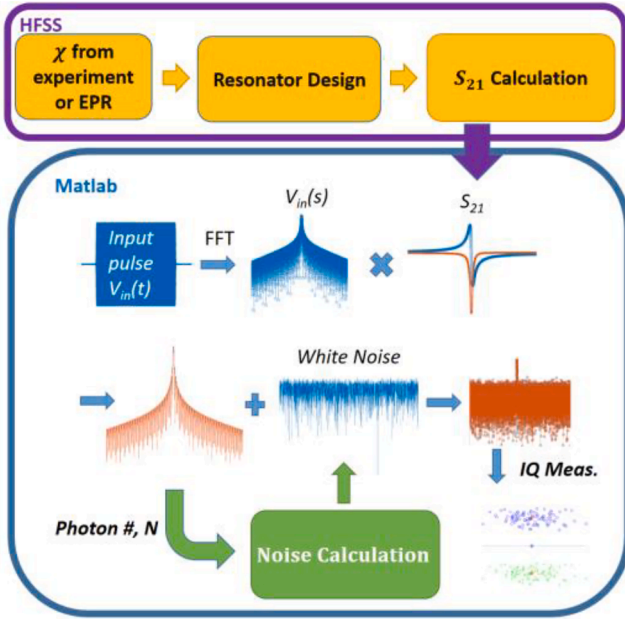


Fig. 2. Illustration of the simulation flow.

input is a single photon [6]. This is equivalent to adding 3 dB of noise to its output. Thirdly, the two low noise amplifiers in Fig. 1 contribute thermal noise equivalent to $T_{eff} = 1.5$ K and $T_{eff} = 54$ K, respectively, with a noise spectral density of $4kT_{eff}R$, where k is the Boltzmann constant and R is 50Ω .

In [7], qubit readout quantum noise (relative to the distance between the $|0\rangle$ and $|1\rangle$ states) was derived based on the qubit relaxation time, resonator photon lifetime, quantum-limited amplifier noise effective temperature, etc. However, this does not allow the inclusion of other noise sources.

To allow the simulation of the quantum noise in our classical framework, the quantum noise due to the photon fluctuation and coming from the TWPA are modeled with white noise [8], and the

fundamental quantum noise limit of a linear amplifier is used based on [9]. The associated equivalent noise temperature, T_n , is computed using the following equation derived in [9],

$$T_n = \frac{1}{\ln 2} \frac{hf}{k} \quad (1)$$

where h , f , and k , are Planck's constant, pulse frequency, and Boltzmann's constant, respectively. A white noise corresponding to T_n is used in the simulation. T_n is found to be 0.5 K.

The white noise power spectral density has a unit of dBm/Hz . It is converted to power in dBm by multiplying by the effective bandwidth, B . For white noises generated at the room temperature and HEMT amplifiers, a bandwidth of 6 GHz is used in the simulation. For the quantum white noise, $B = 1/t_p$ is used.

All noises are generated in the time domain with the calculated noise power and converted into the frequency domain using Fast Fourier Transformation (FFT) to be added to the signal. For the quantum noise, only the noise energy within the pulse time, t_p , should be used because the measurement is only performed over the pulse time in the experiment. It is also assumed that the corresponding noise energy appears at the readout pulse frequency as white noise with a bandwidth of $1/t_p$. Therefore, after FFT of the noise in the simulation, the noise energy in the frequency domain is scaled by $(t_p/T)(F/(1/t_p)) = t_p^2 F/T$, where T and F are the simulation time and frequency domains, respectively. F is also the inverse of the time discretization.

The output pulse from the resonator is simulated by multiplying the attenuated input pulse and the S_{21} of the resonator in the frequency domain. The total noise is then added to the output pulse. The real and imaginary parts at the readout frequency are extracted to simulate the quadrature measurement. 1000 random runs per input state are performed to obtain the statistics, in which the white noise is randomized.

4. Simulation setup

Since the experimental χ is available, the resonators are designed to have eigenfrequencies of 7.252456 GHz and 7.252612 GHz, to emulate the coupled qubit's $|0\rangle$ and $|1\rangle$ states, respectively. This is achieved by designing a resonator length of 3.29265 mm and 3.2925 mm, respectively, without simulating the qubit. A dense mesh is required to achieve the required accuracy. For example, the tips of the resonator have a maximum mesh size of $5 \mu m$. This gives an effective χ of 156 kHz, which is similar to that of the hardware. Fig. 3 shows the design of the cavity and the resonator with $Q \sim 48$ k, similar to the experimental value. If experimental χ is not available, it can be obtained using the Energy Participation Ratio (EPR) method with HFSS [2] for the qubit design and

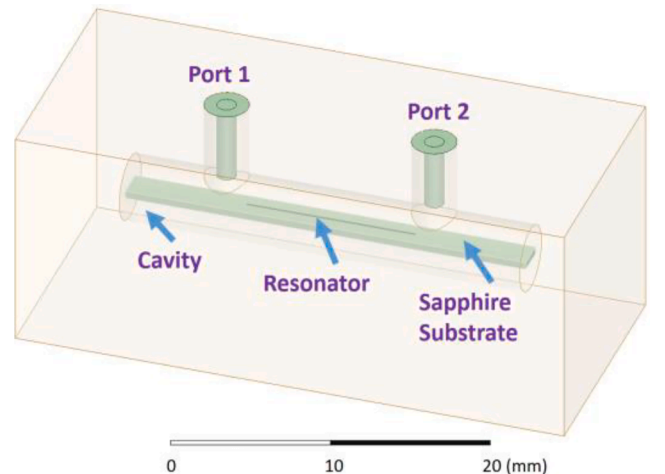


Fig. 3. The cavity and resonator used in the HFSS simulation.

device layout. The readout pulse frequency is $f = 7.252534$ GHz, which is the average of the two resonator frequencies. Based on the simulation, the number of photons entering port 1 is about 363, and 94 photons are emitted from port 2.

Fig. 4 shows the output signal before and after the chain of amplifiers for the resonator coupled with qubit with states $|0\rangle$ and $|1\rangle$. It can be seen that the noise reduces the distinguishability. Note that the amplitude of the bottom figure is larger due to the amplification. The imaginary and real parts are taken at the readout frequency indicated with the red-dashed line to construct the I-Q distribution plots.

5. Simulation results

The framework is then used to predict the fidelity of a -47 dBm readout pulse with $t_p = 3.5 \mu\text{s}$. Fig. 5 shows the fidelity of the qubit readout based on experimental quadrature measurement and simulation. I-Q distributions are plotted for the two qubit states ($|0\rangle$ and $|1\rangle$) for 1000 samples and each I-Q distribution (commonly called “blob”) represents the spreading of the I-Q signal when the qubit is at $|0\rangle$ or $|1\rangle$ state, respectively. The error is calculated by defining the blue axis in the plots as the boundary and counting how many trials are on the wrong side for each input state. It shows that the simulation and experimental results match each other pretty well in terms of $|0\rangle/|1\rangle$ I-Q distribution center distance to I-Q distribution spreading ratio. Note that in the experiment, there are some errors that do not follow the Gaussian distribution (e.g. green cross inside the blue $|0\rangle$ I-Q distribution). They are believed to be qubit reset errors that are dependent on the measurement fidelity and are not captured in the simulation. Before every measurement, the qubit needs to be set up at the correct state. This is done by measuring the qubit first and then applying a setup pulse, if needed, to rotate the qubit to the required state. If this is not done properly, there will be qubit reset errors. In the simulation, this is not simulated.

This framework is then used to study how the input pulse power changes the fidelity of qubit readout. Fig. 6 shows the experiment and simulation readout errors as a function of the relative readout pulse power (relative to -47 dBm). Both simulation and experiment show that the errors increase substantially after -7 dB power reduction (i.e. -54

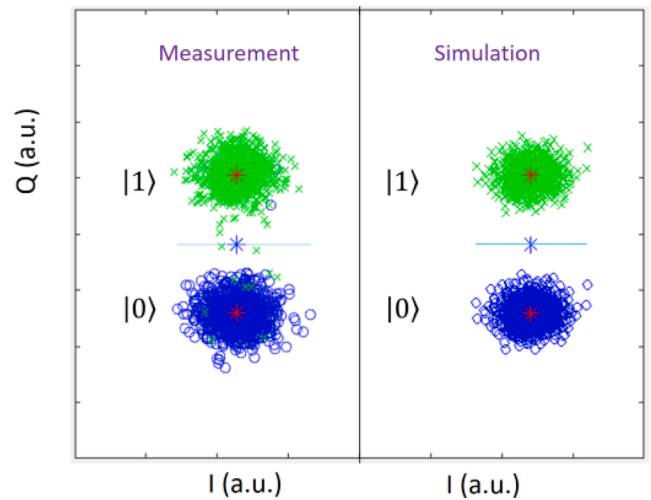


Fig. 5. The quadrature measurement (Left) and simulation (Right) for reading $|0\rangle$ and $|1\rangle$ states, with a -47 dBm readout pulse.

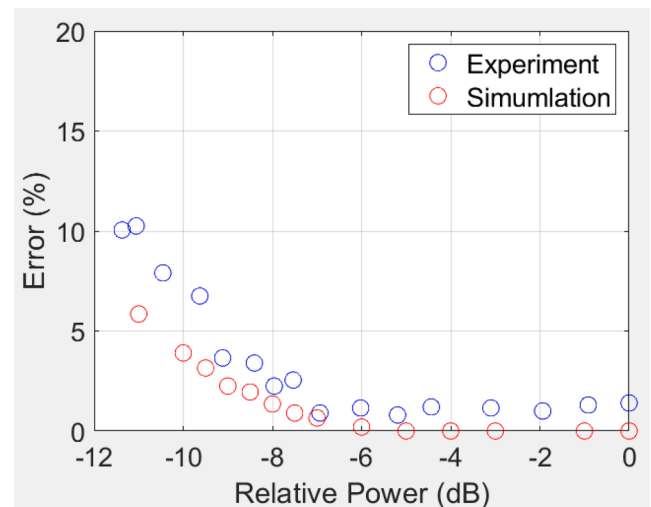


Fig. 6. Simulated and measured readout errors of the qubit readout system as a function of readout pulse power relative to the nominal power.

dBm).

The experiment has non-zero errors at large pulse power due to reset error as mentioned earlier even though the two I-Q distributions have a large separation (Fig. 5). Also, the experiment error increases faster than the simulation one when the power is reduced below -54 dBm, the distributions start to overlap considerably. Fig. 7 shows that the I-Q distributions just touch each other in both the experiment and simulation. Once the I-Q distributions merge, the reading errors increase. For the experiment, the corresponding weaker pulses are used to read the qubit before resetting. Weaker pulses have larger readout error and thus causes more reset errors. The purpose of this simulation is not to match the error quantitatively but to predict when the error will increase substantially. This is because once the error starts increasing when the I-Q distributions merge, the qubit is not suitable for fault-tolerant computation anymore. Therefore, predicting when the I-Q distributions merge is the primary goal.

Fig. 8 shows that the I-Q distributions merge in both the simulation and experiment when the power is 11 dB less than the nominal power. The I-Q distributions have similar overlaps in both the experiment and simulation. However, the experiment has many measurements that are not following the Gaussian distribution and are believed to be reset

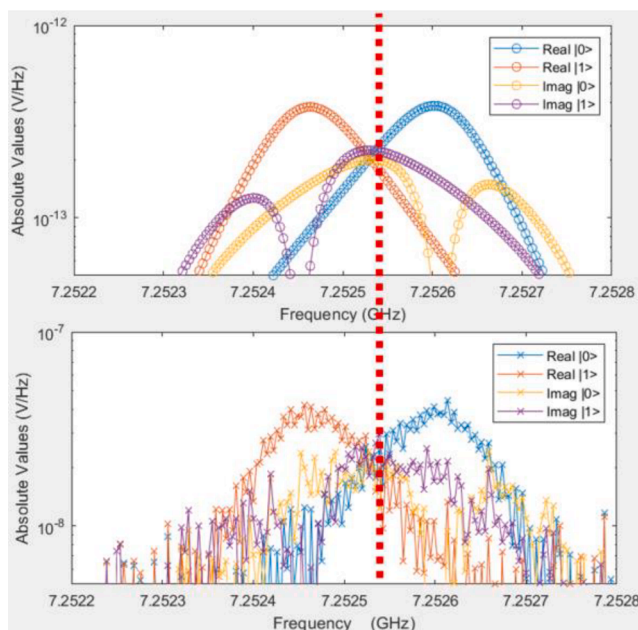


Fig. 4. The real and imaginary components of the signal after the resonator before adding the quantum noise (Top) and after the amplification chain in Fig. 1 (Bottom). The red dotted line indicates the reading pulse frequency. (For interpretation of the references to colour in this figure legend, the reader is referred to the web version of this article.)

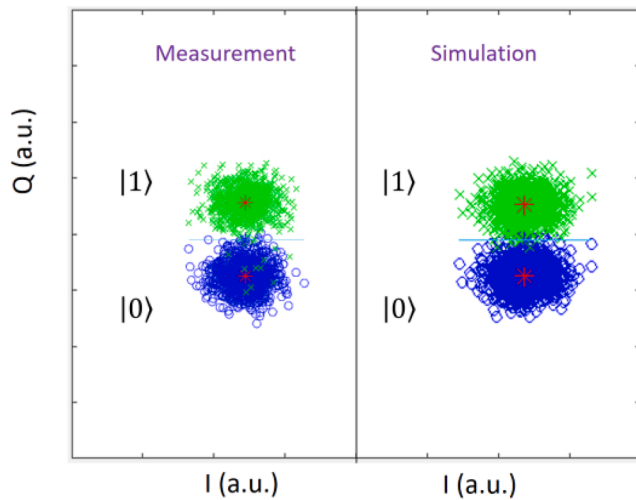


Fig. 7. The quadrature measurement (Left) and simulation (Right) for reading $|0\rangle$ and $|1\rangle$ states, with a -54 dBm (-7 dB less than the nominal power) readout pulse.

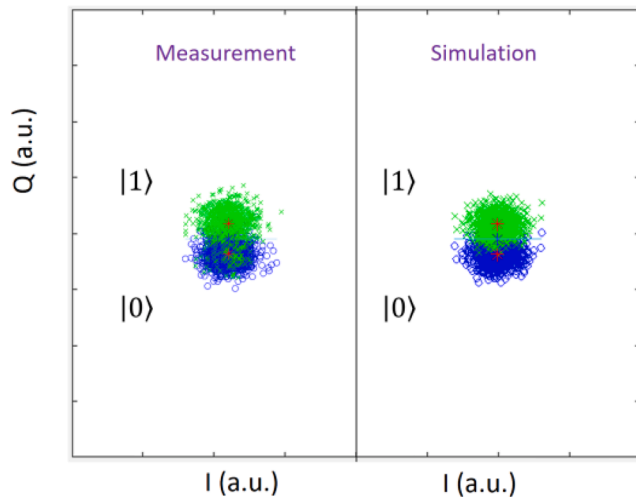


Fig. 8. The quadrature measurement (Left) and simulation (Right) for reading $|0\rangle$ and $|1\rangle$ states, with a -58 dBm (-11 dB less than the nominal power) readout pulse.

errors. Therefore, besides the reset errors, the simulation framework predicts the experimental data well even after the I-Q distributions are overlapped.

6. Conclusions

In this paper, a simulation methodology for predicting superconducting qubit readout fidelity is proposed and implemented using Matlab and HFSS. The quantum noise is treated based on the theory as white noise and the model is able to predict the measurement correctly. Particularly, it can predict how the fidelity changes with the readout pulse power. It is found that the pulse power can be reduced by 7 dB while maintaining high fidelity for the system being studied. The system can thus be further optimized accordingly.

Declaration of Competing Interest

The authors declare the following financial interests/personal relationships which may be considered as potential competing interests: Hiu Yung Wong reports financial support was provided by National Science Foundation.

Data availability

Data will be made available on request.

Acknowledgments

This material is based upon work supported by the National Science Foundation under Grant No. 2125906. The authors thank MITLL and IARPA for allowing us to use their TWPAs. Prepared in part by LLNL under Contract DE-AC52-07NA27344.

References

- [1] Arute F, Arya K, Babbush R, Bacon D, Bardin JC, Barends R, et al. Quantum supremacy using a programmable superconducting processor. *Nature* 2019;574(7779):505–10.
- [2] Mineev ZK, Leghtas Z, Mundhada SO, Christakis L, Pop IM, Devoret MH. Energy-participation quantization of Josephson circuits. *NPJ Quantum Inf* 2021;7(1). <https://doi.org/10.1038/s41534-021-00461-8>.
- [3] <https://www.quantum-machines.co/opx+/>.
- [4] Place APM, Rodgers LVH, Mundhada P, Smitham BM, Fitzpatrick M, Leng Z, et al. New material platform for superconducting transmon qubits with coherence times exceeding 0.3 milliseconds. *Nat Commun* 2021;12(1). <https://doi.org/10.1038/s41467-021-22030-5>.
- [5] Ansys® Academic Research HF, Release 2021 R1.
- [6] <https://www.ibm.com/blogs/research/2020/01/quantum-limited-amplifiers/>.
- [7] David Isaac Schuster. Circuit quantum electrodynamics. Ph.D. thesis. Yale University; 2006.
- [8] Clerk AA, Devoret MH, Girvin SM, Marquardt F, Schoelkopf RJ. Introduction to quantum noise, measurement, and amplification. *Rev Mod Phys* 2010;82(2):1155–208.
- [9] Heffner H. The fundamental noise limit of linear amplifiers. *Proc IRE* 1962;50(7):1604–8.